13.4 W single emitter 940 nm semiconductor laser diode with asymmetric large optical cavity

Jian jun Li (李建军)*, Sheng jie Lin (林盛杰), Tao Liu (刘 涛), Jian chun Li (李佳莼), Jun Deng (邓 军), Jun Han (韩 军), and Bi feng Cui (崔碧峰)

Key Laboratory of Opto-electronics Technology of Ministry of Education,
Beijing University of Technology, Beijing 100124, China
**Corresponding author: lijianjun@bjut.edu.cn*

Received March 26, 2014; accepted May 3, 2014; posted online October 8, 2014

An asymmetric large optical cavity (LOC) waveguide is designed to raise the output power of the 940 nm laser diode. By optimizing the metal organic chemical vapor deposition growth condition and combining with the electrode fabrication and facet coating, single emitter semiconductor laser diodes of 95 μm strip width and 4 mm cavity length are fabricated. Without any active cooling process, an output power of 13.4 W is reached at 15 A injection current without catastrophic optical mirror damage at room temperature. By introducing the asymmetric LOC waveguide, the far-field test shows that only the transverse fundamental mode is lased with a vertical far-field angle full width of half magnitude of 22°.

OCIS codes: 250.5960, 140.0140, 230.7370.
doi: 10.3788/COL201412.S22502.

A 940 nm laser diode (LD) is an efficient pump source of Yb:YAG solid-state lasers[1]. Compared with Nd:YAG, Yb:YAG has an absorption peak at 940 nm. Meanwhile, the line width of the absorption spectrum can be as large as 18 nm. The broad absorption line width means that the wavelength control of the pump diodes is not so strict, so the dimension of the cooling system can be decreased. On the other hand, the emission peak of Yb:YAG is 1030 nm, its doubling wavelength is 515 nm close to that of Ar-ion laser (514 nm), which makes it possible to replace large volume Ar-ion laser.

In order to obtain high optical power from Yb:YAG solid-state laser, efforts have been made to raise the pump power of 940 nm LD. Although the non-absorbing window technique has been adopted to the 940 nm LD, Zhou *et al.* obtained a maximal output power of only 2 W[2]. Erbert *et al.* fabricated an 18 W single emitter 940 nm LD with the strain compensation quantum well structure[3]. Although an optical power of more than 1000 W has been reached for 940 nm LD array[4], the study of single emitter is still the basis to get high-power 940 nm pump source.

We design an asymmetric large optical cavity (LOC) 940 nm LD to improve the limit of catastrophic optical mirror damage (COMD). Although this device has neither strain compensation in active region nor non-absorbing window near facet, a 13.4 W 940 nm single emitter LD is still obtained under room temperature.

Figure 1 shows the epitaxial structure of the 940 nm LD. The active region is a 6 nm $In_{0.15}Ga_{0.85}As$/$Al_{0.15}Ga_{0.85}As$ double quantum well (DQW). An asymmetric LOC is used which consists of a 0.9 μm upper waveguide layer and a 1.2 μm lower waveguide layer. Both upper and lower cladding layers are $Al_{0.35}Ga_{0.55}As$ with a thickness of 0.7 μm and the dopant concentration of 10^{18} cm^{-3}. In order to form ohmic contact, there is a 0.3 μm thick p$^+$-GaAs on upper cladding layer, the dopant concentration near surface is 5×10^{19} cm^{-3}.

GaAs	p:5×10^{19} cm^{-3}	0.3 μm
$Al_{0.35}Ga_{0.65}As$	p:10^{18} cm^{-3}	0.7 μm
$Al_{0.15}Ga_{0.85}As$	i	0.9 μm
$In_{0.15}Ga_{0.85}As$	DQW	
$Al_{0.15}Ga_{0.85}As$	i	1.2 μm
$Al_{0.35}Ga_{0.65}As$	n:10^{18} cm^{-3}	0.7 μm
GaAs buffer	n:10^{18} cm^{-3}	0.2 μm
GaAs substrate	n:10^{18} cm^{-3}	

Fig. 1. Epitaxial structure of 940 nm LD.

Figure 2(a) shows the near-field simulation results of TE_0 along the growth direction. Let d_a be the thickness and Γ_a be the confinement factor of the active region, we obtain the effective field size d_a/Γ_a as 1.16 μm. By using the LOC structure, the size of the transverse field is increased effectively, so that the COMD limit can be improved.

One result of the LOC structure is the increased number of the transverse-guided modes. For the structure shown in Fig. 1, five TE modes may exist within the waveguide, the near-field distribution of each mode is shown in Fig. 2. The problem is how TE_0 mode can only be lased and other higher order modes are suppressed effectively. Which mode among the five will be lased is decided by the following threshold condition:

$$\Gamma_a g_{th} = a_i + (1/L)\ln(1/R), \tag{1}$$

where g_{th} denotes the optical gain in active region, a_i is the cavity loss, L is the cavity length, and R is the

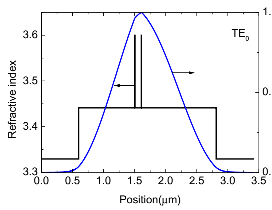

(a) TE_0

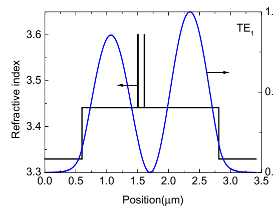

(b) TE_1

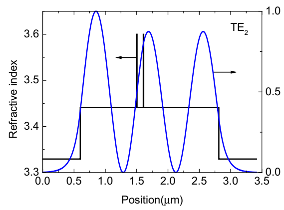

(b) TE_2

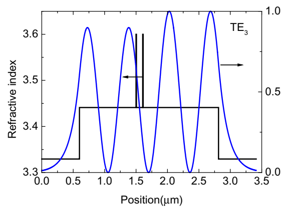

(c) TE_3

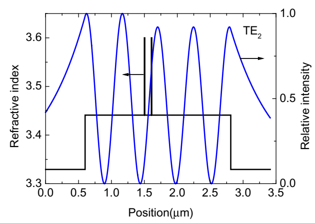

(e) TE_4

Fig. 2. Near-field distribution of each transverse mode in the waveguide.

reflectivity at facets, respectively. According to Eq. (1), when a_i, L, and R are fixed, the mode with the largest Γ_a will have the smallest g_{th}, so the mode will be lased firstly. Here, we use the asymmetric waveguide structure to enlarge the difference in Γ_a between TE_0 mode and other higher order modes. As shown in Table 1, TE_0 has the highest Γ_a among all five modes, so it will be lased firstly.

For the asymmetric LOC, we select the thickness of the lower waveguide larger than that of the upper waveguide because the absorption loss of electron is less than that of the hole[5]. In the lower waveguide, the electron concentration is more than the hole concentration, whereas in the upper waveguide, the situation is reversed. As shown in Fig. 2(a), due to the asymmetric LOC structure, the peak of the TE_0 optical field is shifted toward the lower wave guide, which results in decreased total cavity loss a_i, and lower threshold gain g_{th}.

The epitaxial structure shown in Fig. 1 was grown by EMCORE D125 metal organic chemical vapor deposition system on 2° off (100)-oriented n^+-GaAs substrate. The metal–alkyl sources used are trimethylaluminium, trimethylgallium, and trimethylindium, the hydride precursor gases are pure AsH_3, the carrier gas is H_2 purified by Pd cell, SiH_4 diluted by H_2 and CCl_4 are used as the n- and p-type doping sources, respectively. The optimized growth conditions are growth rate 6 Å/s, growth temperature 675 °C except in active region, that is, 575 °C, the wafer carrier rotation speed 1000 rpm, and growth pressure 80 mbar. After growth, the wafer was evaluated by the photoluminescence (PL) system, as shown in Fig. 3. The peak wavelength is 920 nm and the full width of half magnitude (FWHM) is only 18.3 nm, corresponding to 27 meV, comparable to the thermal energy at room temperature (~26 meV). The PL results indicate that the quality of the epitaxial material is perfect.

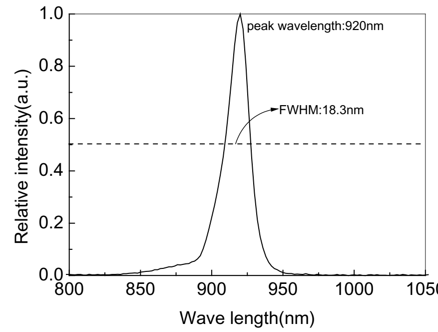

Fig. 3. PL spectrum of epitaxial material.

After epitaxial growth, the electrode was fabricated. A 100 μm wide ridge waveguide with etching depth of 0.6 μm was formed by wet chemical etching. Then, a 200 nm thick SiO_2 was sputtered on the wafer top, the standard photolithograph and etching process were used to form a 95 μm wide strip window for p-electrode. The p-electrode was finished by sputtering a Ti-Au layer on the wafer top. Finally, the n-electrode was formed at a temperature of 400 °C by the evaporation of AuGeNi-Au onto the backside of the substrate, which had been thinned to 130 μm.

Following the alloy process, the wafer was cleaved into 4 mm cavity length bar and coated for the facets, the reflectivity of the back and front facets were 90% and 6%, respectively. After the coated bar was diced into 500 μm wide chip, the chip was soldered p-side down on a C-mount heat sink. At last, the C-mount was mounted on a TO3 socket for measurement.

Figure 4 shows the test result of the optical power versus the injection current at room temperature. Owing to the limited heat dissipation capacity of C-mount, measurement was performed under pulse condition (pulse width = 100 μs, pulse rate = 50 Hz). The device shows a threshold current of 0.28 A, an output power of 13.4 W at 15 A without COMD,

Table 1. Confinement Factor Γ_a of the Active Region for each Mode

	TE_0	TE_1	TE_2	TE_3	TE_4
Γ_a	1.034×10^{-2}	1.255×10^{-3}	6.389×10^{-3}	3.652×10^{-3}	2.028×10^{-3}

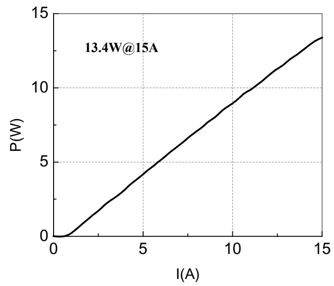

Fig. 4. *P*-*I* characteristics of the 940 nm LD.

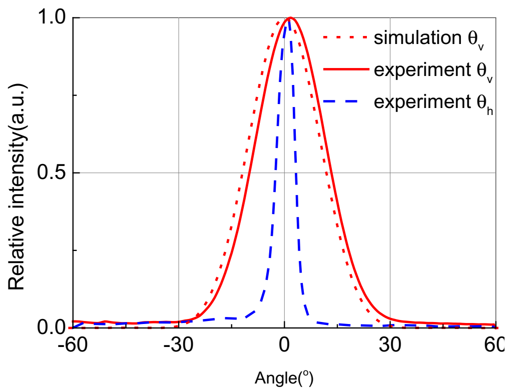

Fig. 5. Experimental and theoretical results of the far-field test.

and a slope efficiency of 0.915 W/A. Figure 5 shows the far-field test results, the FWHM along the junction plane is 5.4°. Because of the LOC structure, the FWHM along the vertical direction is only 22°, which should be about 30° for the normal LD structure[6]. The simulation result of TE_0 is also displayed in Fig. 5, perfect coincidence can be seen between the experiment and the theory, which demonstrates that only the fundamental mode TE_0 along the vertical direction is lased.

The optical spectrum is shown in Fig. 6 for different current ratings of 3, 5, 10, and 15 A. Because of the thermal effect and the limited heat dissipation capacity of C-mount, the peak wavelengths increased with the current, which are 940, 941.6, 944.2, and 946 nm, respectively. Meanwhile, the thermal effect also results in the FWHM increase in the spectrum, which are 1, 1.2, 3, and 3.4 nm, respectively. The results indicate

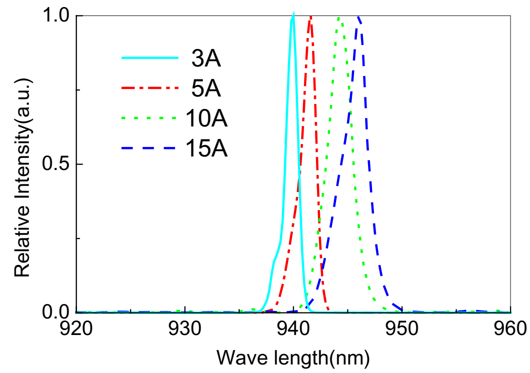

Fig. 6. Spectrum of 940 nm LD at different current rates.

that favorable heat dissipation technique is very important for high-power semiconductor LD.

In conclusion, an asymmetric LOC 940 nm LD is designed and fabricated, in which the LOC structure results in a 13.4 W output power at 15 A without COMD, and the asymmetric waveguide is used to suppress the high-order transverse modes. Meanwhile, the LOC structure decreases the vertical divergence angle to improve the far-field pattern. Based on the relationship between the peak wavelength and the current, the effective heat dissipation technique is essential for high-power semiconductor LDs which work in high injection current.

This work was supported by the Advanced Technology Fund of Beijing University of Technology (No. 002000514312003) and the Beijing Education Committee innovation advancing Projects (No. PXM2013_014204_000029).

References

1. V. V. Ter-Mikirtychev, M. A. Dubinskii, and V. A. Fromzel, Opt. Commun. **197,** 403 (2001).
2. L. Zhou, B. Bo, Y. Wang, B. Jia, D. Bai, Z. Qiao, and X. Gao, Chin. J. Lasers **39,** 0802001 (2012).
3. G. Erbert, F. Bugge, A. Knigge, R. Staske, B. Sumpf, H. Wenzel, and G. Tränkle, Proc. SPIE **6133,** 61330B (2006).
4. R. Diamant, Y. Berk, S. Cohen, G. Klumel, M. Levy, Y. Openhaim, O. Peleg, D. Yanson, and Y. Karni, Proc. SPIE **8039,** 80390E (2011).
5. J. Li, B. Cui, J. Deng, J. Han, T. Liu, J. Li, and S. Zhang Chin. J. Lasers **40,** 1102011 (2013).
6. J. Li, J. Han, J. Deng, D. Zou, and G. Shen, Chin. J. Lasers **33,** 1159 (2006).